

The antithrombotic potential of selective blockade of talin-dependent integrin $\alpha_{IIb}\beta_3$ (platelet GPIIb–IIIa) activation

Brian G. Petrich, ... , Sanford J. Shattil, Mark H. Ginsberg

J Clin Invest. 2007;117(8):2250-2259. <https://doi.org/10.1172/JCI31024>.

Research Article

Hematology

In vitro studies indicate that binding of talin to the β_3 integrin cytoplasmic domain (tail) results in integrin $\alpha_{IIb}\beta_3$ (GPIIb–IIIa) activation. Here we tested the importance of talin binding for integrin activation in vivo and its biological significance by generating mice harboring point mutations in the β_3 tail. We introduced a β_3 (Y747A) substitution that disrupts the binding of talin, filamin, and other cytoplasmic proteins and a β_3 (L746A) substitution that selectively disrupts interactions only with talin. Platelets from animals homozygous for each mutation showed impaired agonist-induced fibrinogen binding and platelet aggregation, providing proof that inside-out signals that activate $\alpha_{IIb}\beta_3$ require binding of talin to the β_3 tail. β_3 (L746A) mice were resistant to both pulmonary thromboembolism and to ferric chloride–induced thrombosis of the carotid artery. Pathological bleeding, measured by the presence of fecal blood and development of anemia, occurred in 53% of β_3 (Y747A) and virtually all β_3 -null animals examined. Remarkably, less than 5% of β_3 (L746A) animals exhibited this form of bleeding. These results establish that $\alpha_{IIb}\beta_3$ activation in vivo is dependent on the interaction of talin with the β_3 integrin cytoplasmic domain. Furthermore, they suggest that modulation of β_3 integrin–talin interactions may provide an attractive target for antithrombotics and result in a reduced risk of pathological bleeding.

Find the latest version:

<https://jci.me/31024/pdf>





The antithrombotic potential of selective blockade of talin-dependent integrin $\alpha_{IIb}\beta_3$ (platelet GPIIb–IIIa) activation

Brian G. Petrich, Per Fogelstrand, Anthony W. Partridge, Nima Yousefi, Ararat J. Ablooglu, Sanford J. Shattil, and Mark H. Ginsberg

Department of Medicine, UCSD School of Medicine, La Jolla, California, USA.

In vitro studies indicate that binding of talin to the β_3 integrin cytoplasmic domain (tail) results in integrin $\alpha_{IIb}\beta_3$ (GPIIb–IIIa) activation. Here we tested the importance of talin binding for integrin activation in vivo and its biological significance by generating mice harboring point mutations in the β_3 tail. We introduced a β_3 (Y747A) substitution that disrupts the binding of talin, filamin, and other cytoplasmic proteins and a β_3 (L746A) substitution that selectively disrupts interactions only with talin. Platelets from animals homozygous for each mutation showed impaired agonist-induced fibrinogen binding and platelet aggregation, providing proof that inside-out signals that activate $\alpha_{IIb}\beta_3$ require binding of talin to the β_3 tail. β_3 (L746A) mice were resistant to both pulmonary thromboembolism and to ferric chloride–induced thrombosis of the carotid artery. Pathological bleeding, measured by the presence of fecal blood and development of anemia, occurred in 53% of β_3 (Y747A) and virtually all β_3 -null animals examined. Remarkably, less than 5% of β_3 (L746A) animals exhibited this form of bleeding. These results establish that $\alpha_{IIb}\beta_3$ activation in vivo is dependent on the interaction of talin with the β_3 integrin cytoplasmic domain. Furthermore, they suggest that modulation of β_3 integrin–talin interactions may provide an attractive target for antithrombotics and result in a reduced risk of pathological bleeding.

Introduction

Primary hemostasis following vascular injury is dependent on the aggregation of platelets and the formation of a platelet plug. In arterial disease, however, platelet aggregation can lead to an occlusive platelet thrombus, resulting in myocardial infarction or stroke. Platelet aggregation requires the binding of soluble multivalent adhesive ligands, such as fibrinogen, fibronectin, or von Willebrand factor to platelet GPIIb–IIIa (integrin $\alpha_{IIb}\beta_3$). Indeed, blockade of ligand binding to $\alpha_{IIb}\beta_3$ by agents such as abciximab, eptifibatide, or tirofiban can completely inhibit platelet aggregation. Thus, these agents are effective in the prevention and treatment of arterial thrombosis in the acute settings of percutaneous coronary intervention (1). In spite of the compelling mechanistic rationale for such pharmacological blockade of $\alpha_{IIb}\beta_3$, the chronic administration of oral $\alpha_{IIb}\beta_3$ antagonists has not proved beneficial in preventing recurrent thrombotic events (2). One plausible explanation for this failure is the relatively narrow therapeutic window for these agents because pathological bleeding associated with complete loss of $\alpha_{IIb}\beta_3$ function necessitates maintenance of less than maximal blockade of the integrin (1). Thus, the role of $\alpha_{IIb}\beta_3$ in arterial thrombosis and the clinical success of acute blockade of this integrin indicate that it is a useful therapeutic target; however, the failure of oral $\alpha_{IIb}\beta_3$ antagonists suggests that a better understanding of how this receptor functions in thrombosis and in prevention of pathological bleeding in vivo could lead to advantageous new approaches to therapeutic platelet inhibition.

Regulation of the affinity of $\alpha_{IIb}\beta_3$ for adhesive ligands is central to the control of platelet aggregation (3). $\alpha_{IIb}\beta_3$ is expressed in a low-

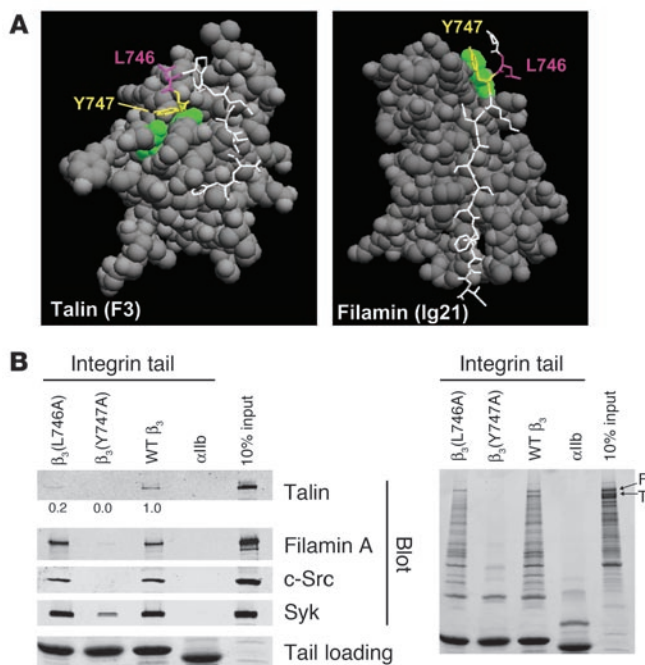
affinity form in resting platelets, and intracellular signals initiated by agonists, such as ADP or thromboxane A_2 , acting via distinct receptors, result in increased affinity of $\alpha_{IIb}\beta_3$, often referred to as “activation” (4). Agents that block signaling through ADP receptors (e.g., clopidogrel) or through the generation of thromboxane A_2 (e.g., aspirin) are moderately beneficial in the chronic prevention of arterial thrombosis (5), suggesting that more effective blockade of the activation of $\alpha_{IIb}\beta_3$ might be a useful antithrombotic strategy.

Activation is an intrinsic property of the integrin $\alpha_{IIb}\beta_3$ and can be due to changes in the conformation of the extracellular domain and/or to cooperative binding to multivalent ligands resulting from integrin clustering (6). Electron microscopic and immunochemical analyses suggest that long-range changes in the tertiary and quaternary structures of integrins also contribute to affinity regulation; however, the full range of these conformational changes remains to be determined (7–9). Recent in vitro analyses, using model systems, indicate that the binding of talin to the cytoplasmic domain of β_3 integrin and other integrin cytoplasmic domains is a final common step in integrin activation (10–12), and they have defined critical structural features of the interaction (13). Taking into consideration insights from these structural studies, we have generated mice with mutations in the mouse β_3 integrin tail that selectively disrupt the binding of talin alone or the binding of talin and several other cytoplasmic proteins to β_3 in platelets. We find that binding of talin to the β_3 integrin tail is critical for agonist-induced $\alpha_{IIb}\beta_3$ activation in vivo. More importantly, we demonstrate that selective disruption of the β_3 integrin–talin interaction protects mice from thrombosis without causing the anemia and gastrointestinal (GI) bleeding associated with the complete loss of β_3 integrin function in β_3 -null mice. These data suggest that disrupting the β_3 -talin interaction may offer antithrombotic benefit by widening the therapeutic window of $\alpha_{IIb}\beta_3$ antagonism.

Nonstandard abbreviations used: GI, gastrointestinal.

Conflict of interest: The authors have declared that no conflict of interest exists.

Citation for this article: *J. Clin. Invest.* 117:2250–2259 (2007). doi:10.1172/JCI31024.

**Figure 1**

Structure-based mutagenesis of the β_3 integrin cytoplasmic domain. (A) Space-filled models of talin F3 domain (left) or filamin A immunoglobulin-like domain 21 in complex with short internal fragments of the β_3 integrin cytoplasmic domain (shown as sticks, with Tyr747 and Leu746 in yellow and purple, respectively). (B) Affinity chromatography using recombinant WT and mutant β_3 cytoplasmic domain proteins and mouse platelet lysates as described in Methods. Bound platelet proteins were analyzed by Western blotting with the indicated antibodies (left panel) and by Coomassie blue staining (right panel). Quantitation of the amount of talin bound in mutant relative to WT platelets is shown. Similar results were obtained from 2 independent experiments. F, filamin; T, talin.

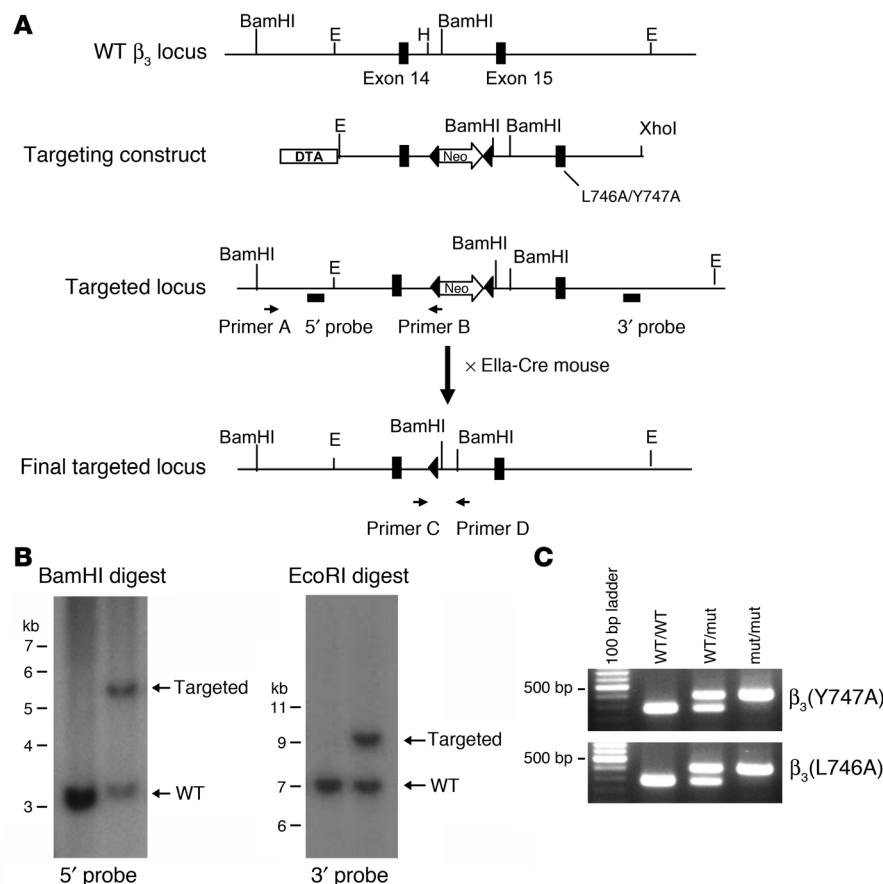
murine platelet function of selective blockade of talin binding versus a more general blockade of protein interactions.

Generation of mice bearing β_3 (Y747A) and β_3 (L746A) mutations. To test the effects of β_3 (Y747A) and β_3 (L746A) mutations on platelet function, we generated mice harboring either of these mutations using a gene-targeting approach similar to that previously described for the construction of the β_3 (Y747,759F) integrin subunit (16). Mouse 129/SvJ ES cells were electroporated with a targeting vector containing 6 kb of β_3 genomic sequence, a *loxP*-flanked neomycin (Neo) cassette inserted between exons 14 and 15, and either Y747A or L746A mutation in exon 15 (Figure 2A). ES clones were screened by PCR and confirmed by Southern blotting using cDNA probes 5' and 3' to the targeted sequence (Figure 2B) and with a Neo probe to confirm a single integration site of the targeting vector (data not shown). For each mutation, 2 independently derived clones of ES cells were injected into C57BL/6 blastocysts. Each ES cell clone generated chimeric mice that exhibited germline transmission of the mutation as determined by PCR (data not shown). Heterozygous animals were crossed with EIIa-Cre mice to obtain offspring in which the Neo cassette was excised. Heterozygous animals were crossed to obtain animals homozygous for the mutations or WT littermates as determined by PCR on genomic DNA isolated from ear biopsy samples (Figure 2C). The presence of the mutation in β_3 integrin mRNA was confirmed by sequencing reverse transcription-polymerase chain reaction products generated using RNA isolated from spleens of homozygous mutant animals. Mice were backcrossed to a C57BL/6 strain for at least 3 generations, and WT sex-matched littermates were used as controls for homozygous mutant animals in all experiments. Similar to β_3 -null animals (17), these mutant mice exhibited no gross developmental abnormalities and had normal platelet and white blood cell counts (Table 1). Thus, the mice are suitable for examination of blocking interactions of the β_3 cytoplasmic domain on platelet function in vivo and in vitro.

Protection from thrombosis in β_3 (Y747A) and β_3 (L746A) mice. Since $\alpha_{IIb}\beta_3$ is required for platelet aggregation, we examined the effect of the β_3 (Y747A) and β_3 (L746A) mutations on the formation of occlusive platelet thrombi in a pulmonary thromboembolism model in which platelet activation was induced by tail vein infusion of collagen and epinephrine. Upon intravenous injection of a mixture of these platelet agonists, 64% of WT littermates (20 of 31 mice) died within 5 minutes (Figure 3A). Histological examination of lung tissue from these animals revealed platelet thrombi throughout the pulmonary vasculature (Figure 3B). In sharp contrast, 100% of β_3 (Y747A) (12 of 12 mice) and 95% of β_3 (L746A) (15 of 16 mice) animals survived the infusion of collagen and epinephrine ($P < 0.005$,

Results

Integrin β_3 cytoplasmic domain mutants that disrupt interactions with platelet intracellular proteins. Previous in vitro studies with human proteins pointed to β_3 (Tyr747) and β_3 (Leu746) as potential targets for disrupting the intracellular interactions of the β_3 cytoplasmic domain with talin (13, 14). The crystal structure of β_3 residues Trp739 to Tyr747 in complex with talin F3 shows that both β_3 (Tyr747) and β_3 (Leu746) make extensive contacts with talin. In contrast, a homology model of β_3 (Pro745 to Ile757) docked into the structure of filamin A immunoglobulin-like domain 21 predicted hydrophobic contacts between β_3 (Tyr747) and a loop between 2 β strands in filamin A. However, in contrast to what occurs in the integrin-talin interaction, β_3 (Leu746) makes no contacts with filamin A (Figure 1A). These structures explain why β_3 (Y747A) blocks the binding of both human talin and filamin, whereas β_3 (L746A) blocks only talin binding (12). To test the role of β_3 (Tyr747) and β_3 (Leu746) on the binding of proteins from murine platelet lysates, we used recombinant WT and mutant β_3 integrin cytoplasmic domain proteins in affinity chromatography experiments. WT β_3 bound mouse talin and filamin. In addition, the β_3 cytoplasmic domain bound the tyrosine kinases Syk and c-Src (Figure 1B, left panel). β_3 (Y747A) disrupted interactions with each of these mouse proteins. In sharp contrast, although β_3 (L746A) bound much less talin than WT β_3 , it bound other proteins to the same extent as WT β_3 . Inspection of protein-stained gels underscored the specificity of the effect of the β_3 (L746A) mutation on protein binding; there was no substantial reduction in any of the β_3 -binding proteins other than talin (Figure 1B, right panel). These results indicate that both β_3 (Y747A) and β_3 (L746A) mutations disrupt β_3 -talin interactions in mouse platelets. However, β_3 (Y747A) blocks binding of many other proteins, probably because it disrupts the β turn formed by N⁷⁴⁴PLY (15) in addition to disrupting direct contacts with the protein ligands. Thus, the effects of these point mutations on the binding of murine proteins to the β_3 cytoplasmic domain enable us to evaluate the effects on

**Figure 2**

Generation of β_3 (Y747A) and β_3 (L746A) mutant mice. **(A)** Targeting vector containing 6 kb of the 3' end of the mouse β_3 integrin gene (exons 14 and 15). Tyr747- and Leu746-to-alanine mutations were inserted into exon 15. DTA, diphtheria toxin A. **(B)** Southern blot analysis of R1 ES cell genomic DNA transfected with the β_3 (Y747A) targeting vector digested with BamHI (left) or EcoRI (right) using a 5' probe or 3' probe, respectively. **(C)** PCR genotyping of genomic DNA isolated from β_3 (Y747A) and β_3 (L746A) mouse ear biopsy samples using primers C and D shown in **A**. H, HindIII; E, EcoRI.

able blood in their stool (Figure 5A). In contrast, fewer β_3 (Y747A) animals (19 of 36) were positive for fecal blood, indicating that β_3 (Y747A) impairs vascular integrity to a lesser extent than complete lack of β_3 . In sharp contrast to the results in null and β_3 (Y747A) mice, less than 5% of β_3 (L746A) animals (1 of 23) exhibited fecal blood. The protection from GI bleeding in the β_3 (L746A) mice was confirmed by their lack of anemia relative to the β_3 (Y747A) animals (Figure 5B and Table 1). Indeed, β_3 (L746A) mice showed hematocrits and hemoglobin levels similar to those of WT animals. The pathological bleeding observed in β_3 (Y747A) mice was associated with reduced prenatal

WT versus either mutant; Figure 3A). The lungs of these mutant mice were largely devoid of platelet thrombi (Figure 3B).

To examine the effects of the β_3 (L746A) mutations in a model of arterial thrombosis initiated by vascular injury, we measured the time course of thrombus formation in response to ferric chloride-induced injury of the common carotid artery. In this model, the carotid arteries of 6 of 6 WT mice completely occluded in an average of 6.4 ± 1.9 minutes following injury (Figure 4A). In contrast, arteries of 0 of 5 β_3 (L746A) mice occluded during the 30 minutes following injury despite similar levels of ferric chloride-induced endothelial damage (Figure 4, A and B). Thus, β_3 (L746A) mice are protected from thrombosis in models involving impact to large arteries or the microcirculation.

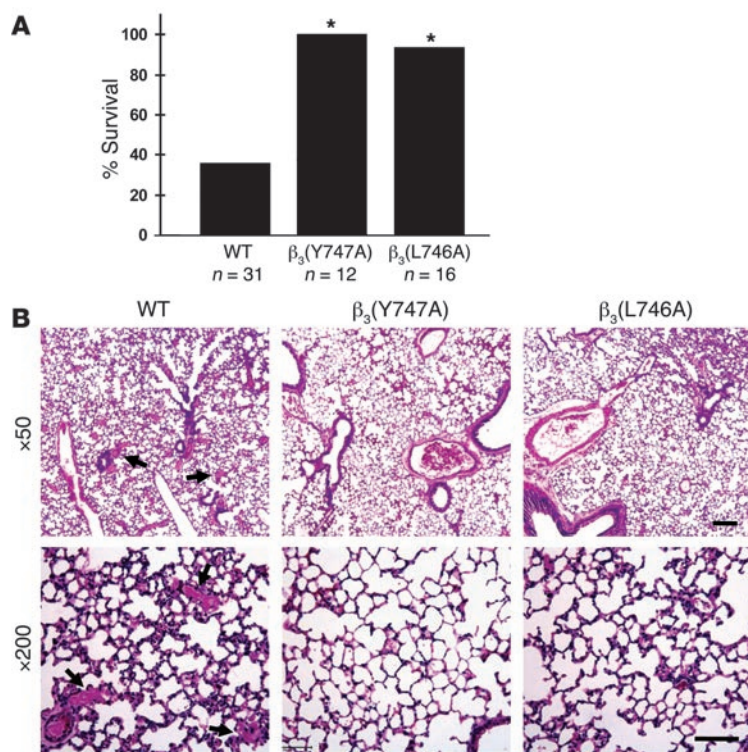
Reduced GI bleeding in β_3 (L746A) mice. Mice entirely lacking integrin β_3 exhibit GI bleeding associated with reduced survival (17). Indeed, in our hands 100% (11 of 11) of β_3 -null animals had detect-

and perinatal survival. Significantly fewer homozygous β_3 (Y747A) mutant animals obtained from heterozygote by heterozygote breedings survived to weaning age (144 homozygotes versus 192 WT; $P < 0.00001$). β_3 (L746A) animals, however, were observed at expected Mendelian ratios (106 homozygotes versus 108 WT; $P = 0.97$). Together, these results indicate that β_3 (Y747A) animals display a

Table 1
Hemograms for WT and β_3 mutant mice

| | β_3 (L746A) | | | | β_3 (Y747A) | | | |
|-------------------------------|-------------------|-----|-------------------|-----|-------------------|-----|-------------------|-----|
| | WT | | Homozygous | | WT | | Homozygous | |
| | Mean | SEM | Mean | SEM | Mean | SEM | Mean | SEM |
| wbc ($\times 10^9$ /l) | 4.2 | 0.4 | 3.2 | 0.3 | 4.2 | 0.9 | 2.6 | 0.3 |
| rbc ($\times 10^9$ /l) | 9.0 | 0.1 | 8.2 ^A | 0.2 | 9.1 | 0.2 | 6.8 ^A | 0.4 |
| Hemoglobin (g/l) | 13.9 | 0.1 | 13.3 | 0.3 | 13.8 | 0.3 | 10.8 ^A | 0.6 |
| Hematocrit (%) | 49.1 | 0.7 | 46.7 | 1.1 | 48.4 | 0.6 | 39.8 ^A | 2.2 |
| MCV (fl) | 54.4 | 0.6 | 56.8 | 1.3 | 53.5 | 0.8 | 58.5 ^A | 0.9 |
| MCH (pg) | 15.4 | 0.1 | 16.2 ^A | 0.2 | 15.2 | 0.1 | 16.0 ^A | 0.3 |
| MCHC (g/dl) | 28.4 | 0.3 | 28.6 | 0.5 | 28.5 | 0.5 | 27.4 | 0.5 |
| Platelets ($\times 10^9$ /l) | 618 | 57 | 616 | 57 | 633 | 69 | 689 | 51 |
| Neutrophils (%) | 41.5 | 3.8 | 39.8 | 5.7 | 32.5 | 4.0 | 36.7 | 5.0 |
| Lymphocytes (%) | 47.9 | 4.4 | 50.5 | 6.4 | 53.1 | 4.5 | 53.4 | 5.4 |
| Monocytes (%) | 6.8 | 1.1 | 6.5 | 1.0 | 9.5 | 1.0 | 7.2 | 0.9 |
| Eosinophils (%) | 3.4 | 0.7 | 3.3 | 0.8 | 5.1 | 1.1 | 2.8 | 0.9 |

^A $P < 0.05$ versus WT. MCV, mean corpuscular volume; MCH, mean corpuscular hemoglobin; MCHC, MCH concentration.

**Figure 3**

β_3 (Y747A) and β_3 (L746A) mice are protected from microvascular thrombosis. (A) Mice were injected intravenously with 800 µg/kg collagen and 60 µg/kg epinephrine and monitored for 30 minutes. * $P < 0.005$. (B) Representative sections of H&E-stained lungs from a WT mice that died during the assay and β_3 (Y747A) and β_3 (L746A) mice that survived and were sacrificed immediately following the assay. WT sections show extensive microthrombi throughout the lungs, while β_3 mutant lungs were clear. Scale bars: 200 µm (upper panel); 100 µm (lower panel).

bleeding diathesis similar to that reported for β_3 -null animals. On the other hand, β_3 (L746A) mice were much less predisposed to these pathologies or to reduced survival.

The foregoing results indicated that the β_3 (L746A) mice were protected from thrombosis yet were spared the frequent occurrence of GI bleeding and reduced survival observed in β_3 (Y747A) and β_3 -null mice. To examine the ability of these animals to achieve hemostasis following injury, we measured the time required to arrest bleeding following tail resection. Both β_3 (Y747A) and β_3 (L746A) animals manifested impaired hemostasis as evidenced by failure to arrest bleeding within 10 minutes compared with an average of 90 seconds in WT animals (Figure 5C). Thus, while spontaneous GI bleeding is markedly reduced in β_3 (L746A) animals, both β_3 (Y747A) and β_3 (L746A) animals showed impaired hemostasis in a tail bleeding assay.

Disrupted inside-out signaling in platelets from β_3 mutant mice. To explore the cellular basis for the biological effects of the β_3 (Y747A) and β_3 (L746A) mutations in mice, we evaluated agonist-induced activation of $\alpha_{IIb}\beta_3$ by measuring fibrinogen binding to platelets. As expected, WT β_3 mice showed a large increase in the amount of specifically bound fibrinogen in response to ADP/epinephrine, PMA, or a PAR4 thrombin receptor agonist peptide (Figure 6A). β_3 (Y747A) and β_3 (L746A) platelets showed profoundly impaired responses. In contrast, β_3 (Y747A) and β_3 (L746A) platelets bound fibrinogen somewhat better than WT β_3 platelets in the presence of 0.5 mM $MnCl_2$, an exogenous activator of the integrin (Figure 6B, left panel). This increased binding was accounted for by a modest increase in β_3 integrin surface expression in β_3 (Y747A) and β_3 (L746A) compared with control platelets (Figure 6B, right panel). Neither platelets preincubated with the β_3 -blocking antibody 1B5 nor β_3 -null platelets bound fibrinogen in response to the agonists, indicating that the fibrinogen binding was depen-

dent on the β_3 integrin (data not shown). Consistent with the fibrinogen-binding defects observed, agonist-induced platelet aggregation was impaired in both mutants (Figure 6C). It is noteworthy that similar functional impairments were observed with selective disruption of talin binding to β_3 (L746A) and a near complete blockade of cytoplasmic protein binding to β_3 (Y747A). This provides additional evidence for the critical and selective role of talin in this process. Thus, these mutant $\alpha_{IIb}\beta_3$ integrins are defective in their capacity to respond with increased affinity to intracellular signals rather than in their innate capacity to bind fibrinogen.

Consistent with preservation of $\alpha_{IIb}\beta_3$ ligand-binding function, static adhesion of platelets to immobilized fibrinogen was similar in WT, β_3 (Y747A), and β_3 (L746A) platelets (Figure 6D). Platelet adhesion was markedly reduced by 1B5, an $\alpha_{IIb}\beta_3$ -blocking antibody, or in β_3 -null platelets, indicating that adhesion is dependent on β_3 integrins. These results show that β_3 integrins expressed on β_3 (Y747A) and β_3 (L746A) platelets maintain ligand-binding function and confirm a previous report that $\alpha_{IIb}\beta_3$ activation is not required for static adhesion of platelets to fibrinogen (18).

Intact outside-in signaling in platelets from β_3 (L746A) mice. Once integrins have bound ligand, they can generate biochemical responses, such as activation of Src family kinases and tyrosine phosphorylation of focal adhesion kinase phosphoprotein of 125 kD (pp125^{FAK}), that result in cell spreading. To examine the ability of β_3 (L746A) to mediate this form of signaling, termed *outside-in* signaling, we measured tyrosine phosphorylation of pp125^{FAK} in response to fibrinogen binding to platelets. When washed platelets were resuspended in buffer containing 250 µg/ml fibrinogen and stimulated by addition of 100 µM ADP/100 µM epinephrine, WT platelets, but not platelets from β_3 (L746A) animals, showed an increase in pp125^{FAK} phosphorylation (Figure 7). However, in the presence of 0.5 mM $MnCl_2$ to activate $\alpha_{IIb}\beta_3$ extrinsically, β_3 (L746A) platelets exhibited fibrinogen-dependent pp125^{FAK} phosphorylation similar to that of WT platelets. This indicates that $\alpha_{IIb}\beta_3$ (L746A) is able to mediate outside-in signaling when ligated by fibrinogen. Thus, the reduced pp125^{FAK} phosphorylation in β_3 (L746A) platelets shown in Figure 7 is ascribable to their failure to increase fibrinogen binding in response to ADP/epinephrine. β_3 (L746A) platelets showed reduced spreading on fibrinogen in response to ADP or PMA (Figure 8). In the presence of $MnCl_2$, however, spreading was similar in WT and β_3 (L746A) platelets. Together, these data indicate that blocking talin binding to β_3 inhibits $\alpha_{IIb}\beta_3$ activation but maintains outside-in signaling and platelet spreading if the $\alpha_{IIb}\beta_3$ is activated exogenously.

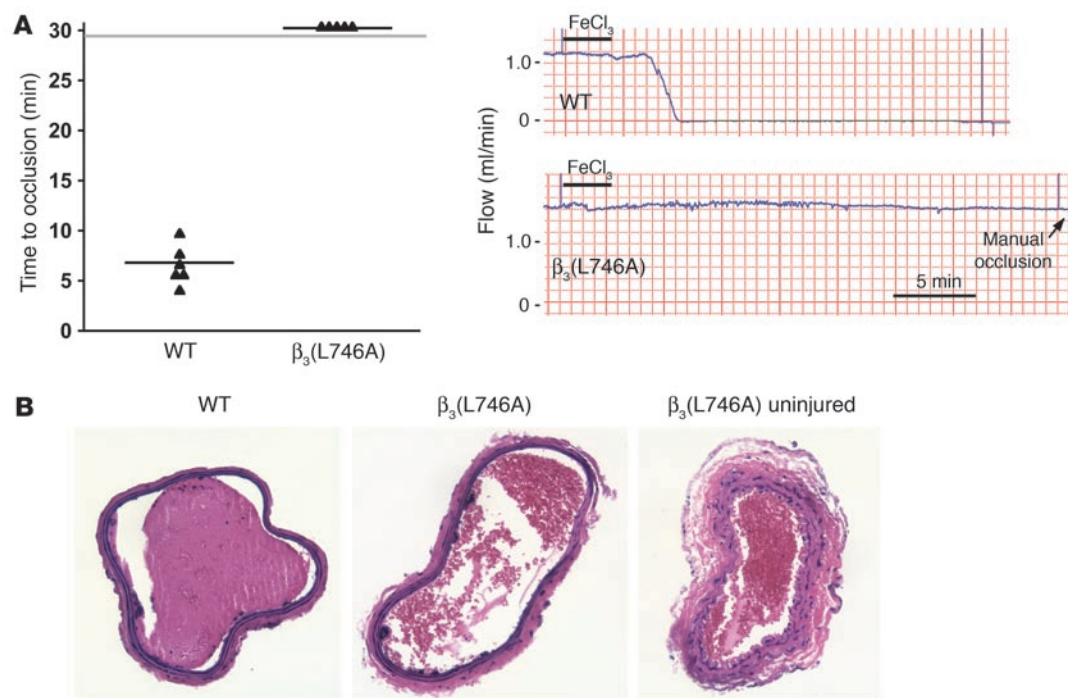


Figure 4

β_3 (L746A) mice are protected from arterial thrombosis. **(A)** Thrombosis was induced in the carotid artery of mice by a 3-minute application of 5% ferric chloride to the surface of the vessel. The time to complete vessel occlusion was considered the time after injury to zero blood flow as measured with a Doppler flow probe. Representative Doppler flow tracings from a WT and a β_3 (L746A) mouse are shown. **(B)** H&E-stained sections of carotid arteries of WT and β_3 (L746A) mice obtained 30 minutes after ferric chloride injury. A section of β_3 (L746A) carotid artery distal to the injury is shown for comparison. Original magnification, $\times 200$.

Discussion

Here we have tested the importance of talin binding to integrin β_3 in the activation of platelet $\alpha_{IIb}\beta_3$ and in hemostasis and thrombosis. Guided by insights derived from structural studies of the interactions between the β_3 integrin cytoplasmic domain and cytoplasmic proteins, we have generated 2 mouse strains bearing β_3 mutations that disrupt talin binding. One strain bears β_3 (Y747A), a mutation that disrupts multiple protein interactions with the β_3 integrin cytoplasmic domain; the second bears β_3 (L746A), a mutation that selectively disrupts β_3 integrin–talin interactions. Both strains of mutant mice were protected from pulmonary thrombosis following intravenous injection of collagen and epinephrine. In addition, β_3 (L746A) animals showed protection from ferric chloride–induced thrombosis of the carotid artery. Thus, using 2 distinct models of thrombosis, we have established that inhibition of the talin– β_3 interaction confers an antithrombotic effect. In contrast, β_3 (L746A) mice were relatively resistant to the pathological bleeding, as assessed by GI blood loss and anemia, that occurred in 53% of β_3 (Y747A) and virtually all β_3 -null mice (Figure 5 and ref. 17). Platelets from both β_3 (Y747A) and β_3 (L746A) mice showed marked reduction in agonist-induced fibrinogen binding to $\alpha_{IIb}\beta_3$, providing what we believe to be the first in vivo evidence for the talin dependence of integrin activation in mammals. However, platelet adhesion to immobilized fibrinogen under static conditions was unaffected by either β_3 cytoplasmic domain mutation, demonstrating that the $\alpha_{IIb}\beta_3$ in β_3 (Y747A) and β_3 (L746A) platelets maintains $\alpha_{IIb}\beta_3$ ligand binding function. While both mutants showed disrupted activation of $\alpha_{IIb}\beta_3$, platelets from the β_3 (L746A)

mice were able to spread on fibrinogen and exhibit tyrosine phosphorylation of pp125^{FAK} when $\alpha_{IIb}\beta_3$ was activated exogenously by MnCl_2 . Thus, β_3 (L746A) mice have a selective defect in the inside-out signaling required for activation of $\alpha_{IIb}\beta_3$, yet their platelets maintain the capacity to generate $\alpha_{IIb}\beta_3$ -mediated outside-in signals required for platelet spreading. Together, these results establish the importance of the talin– β_3 integrin interaction in $\alpha_{IIb}\beta_3$ activation in platelets and show that blocking this interaction can have a potent antithrombotic effect without the kind of pathological bleeding associated with complete lack of $\alpha_{IIb}\beta_3$ function.

Previous studies using a variety of in vitro approaches showed that talin binding to the β_3 integrin cytoplasmic domain induces $\alpha_{IIb}\beta_3$ activation (10, 11) and is a final common step in the process (12). Platelets bearing β_3 (L746A), which leads to specific loss of talin binding, bound significantly less fibrinogen in response to platelet agonists than WT platelets, indicating a marked defect in inside-out signaling (Figure 6). The low levels of fibrinogen binding observed with high agonist doses in β_3 (L746A) and β_3 (Y747A) mutant platelets may have been due to either incomplete inhibition of talin binding to the integrin or to the existence of a talin-independent $\alpha_{IIb}\beta_3$ activation mechanism. Truncation of the β_3 cytoplasmic domain [β_3 (724X); ref. 19] or a point mutation [β_3 (S752P)] (20) is associated with defective hemostasis and reduced agonist-mediated $\alpha_{IIb}\beta_3$ activation in humans; however, the β_3 (724X) mutation is expected to block binding of multiple proteins (21), and the binding defect in β_3 (S752P) remains to be defined (22). Furthermore, in contrast to β_3 (L746A), the 2 human mutations impair outside-in signaling (23, 24). Our results are

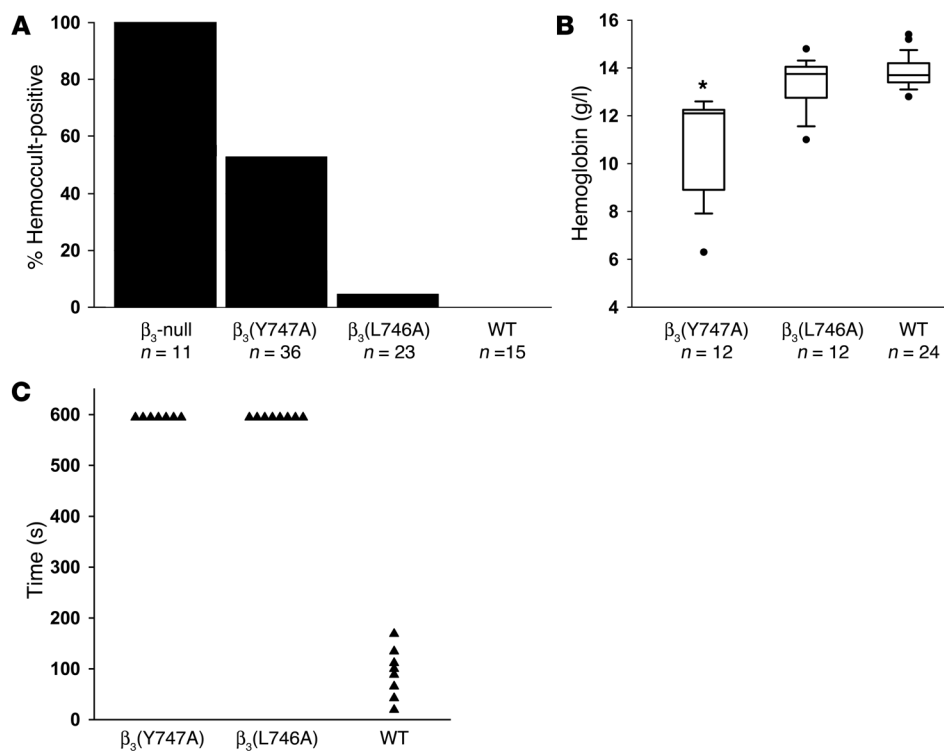


Figure 5

Bleeding diathesis in β_3 mutant mice. **(A)** The presence of fecal blood was detected using a guaiac-based hemocult test. Fecal specimens obtained from the indicated genotypes of mice at 6–12 weeks of age were scored as positive or negative in a blinded manner. **(B)** Box plot showing hemoglobin concentration measured in peripheral blood. Filled circles represent outliers and were included in statistical analysis. * $P < 0.05$ compared with WT. **(C)** Tail bleeding times. β_3 (Y747A) and β_3 (L746A) homozygotes showed bleeding times of at least 10 minutes (at which time bleeding was stopped by cauterization), while WT mice showed significantly shorter bleeding times.

complemented by the subtle hemostatic and platelet function defects observed in mice bearing β_3 (Y747,759F) mutations. Those mice display a defect in secondary platelet aggregation ascribed to defective outside-in signaling and manifest rebleeding from tail wounds after initial hemostasis (16). The β_3 (Y747,759F) mutation does not block talin binding, and platelets from those animals manifested normal agonist-induced activation of integrin $\alpha_{IIb}\beta_3$ and primary hemostasis. In contrast, as noted above, the β_3 (L746A) and β_3 (Y474A) mice showed defective $\alpha_{IIb}\beta_3$ activation, impaired primary aggregation, and prolonged bleeding times. Because of these differences in functional effects, it would be of great interest to examine the impact of the β_3 (Y747,759F) mutations in comparison to the dramatic effect of the β_3 (L746A) mutation on platelet-dependent thrombosis.

The importance of talin binding for integrin activation in vivo is likely to apply to other integrins. The critical structural features for talin binding are conserved in multiple mammalian (β_1 , β_2 , β_3 , β_5 , β_6 , β_7) integrins and in invertebrate integrins (13). Previous in vitro studies indicate that talin participates in the activation of β_1 and β_2 integrins (12, 25, 26). Mice bearing β_1 (Y783,795A) manifest defective β_1 integrin activation in keratinocytes and platelets (27, 28). β_1 (Y783A) is known to disrupt talin binding to β_1 (14); hence, the defective activation of β_1 (Y783,795A) integrins is consistent with a general role for talin in activation of β_1 integrins in vivo. Nevertheless, as shown in Figure 1, a tyrosine-to-alanine substitution at this position within the β_3 integrin (or a homologous mutation in β_1 integrin; ref. 14) disrupts many protein interactions with the β integrin cytoplasmic domain. Thus, the results from the β_3 (L746A) mutant mouse reported here, harboring a mutation that selectively disrupts β_3 integrin–talin interactions, unambiguously demonstrate that talin binding to the integrin β cytoplasmic domain is critical for in vivo integrin activation.

Blockade of talin binding to $\alpha_{\text{IIb}}\beta_3$ inhibits thrombosis with less pathological bleeding than complete lack of $\alpha_{\text{IIb}}\beta_3$ function. Loss of $\alpha_{\text{IIb}}\beta_3$ in humans, due to mutation in either α_{IIb} or β_3 integrin genes (Glanzmann thrombasthenia) or as the result of pharmacological blockade of ligand binding to $\alpha_{\text{IIb}}\beta_3$, is associated with an increased risk of pathological bleeding (1, 29). Gene-targeted mice lacking $\alpha_{\text{IIb}}\beta_3$ are protected from thrombosis (30) but manifest a greater than 95% incidence of GI bleeding and are severely anemic (ref. 17 and Figure 5). β_3 (L746A) animals displayed negligible GI bleeding or anemia (Figure 5). The ability of β_3 (L746A) platelets to adhere to immobilized fibrinogen and to generate outside-in signals may account for the lack of pathological bleeding. The increased GI bleeding in the β_3 (Y747A) mice is likely a reflection of the lack of selectivity of β_3 (Y747A) for inhibition of binding of cytoplasmic proteins, implying that β_3 (Y747A) can disrupt many signaling events in addition to integrin activation (31, 32). Whereas β_3 (L746A) animals showed little sign of pathological bleeding, they, like β_3 (Y747A) and β_3 -null animals, displayed impaired hemostasis in response to tail resection. In β_3 (L746A) mice, agonist-induced fibrinogen binding, a key step in aggregation, was blocked, and tail resection resulted in bleeding from medium-sized veins and arteries. Thus, $\alpha_{\text{IIb}}\beta_3$ -mediated platelet aggregation is essential for arrest of bleeding from larger vessels, but the $\alpha_{\text{IIb}}\beta_3$ -mediated adhesion and outside-in signaling may be sufficient for hemostasis in the microcirculation.

The results of this study suggest that blockade of the talin- $\alpha_{IIb}\beta_3$ interaction may offer a therapeutic target in pathological thrombosis. Because ligand binding to integrin $\alpha_{IIb}\beta_3$ is absolutely required for platelet aggregation, $\alpha_{IIb}\beta_3$ inhibitors are an effective monotherapy for preventing acute thrombosis in the setting of percutaneous coronary intervention (33). In sharp contrast, chronic blockade of $\alpha_{IIb}\beta_3$ by orally administered antagonists is ineffective in thrombosis protection, possibly because of the need

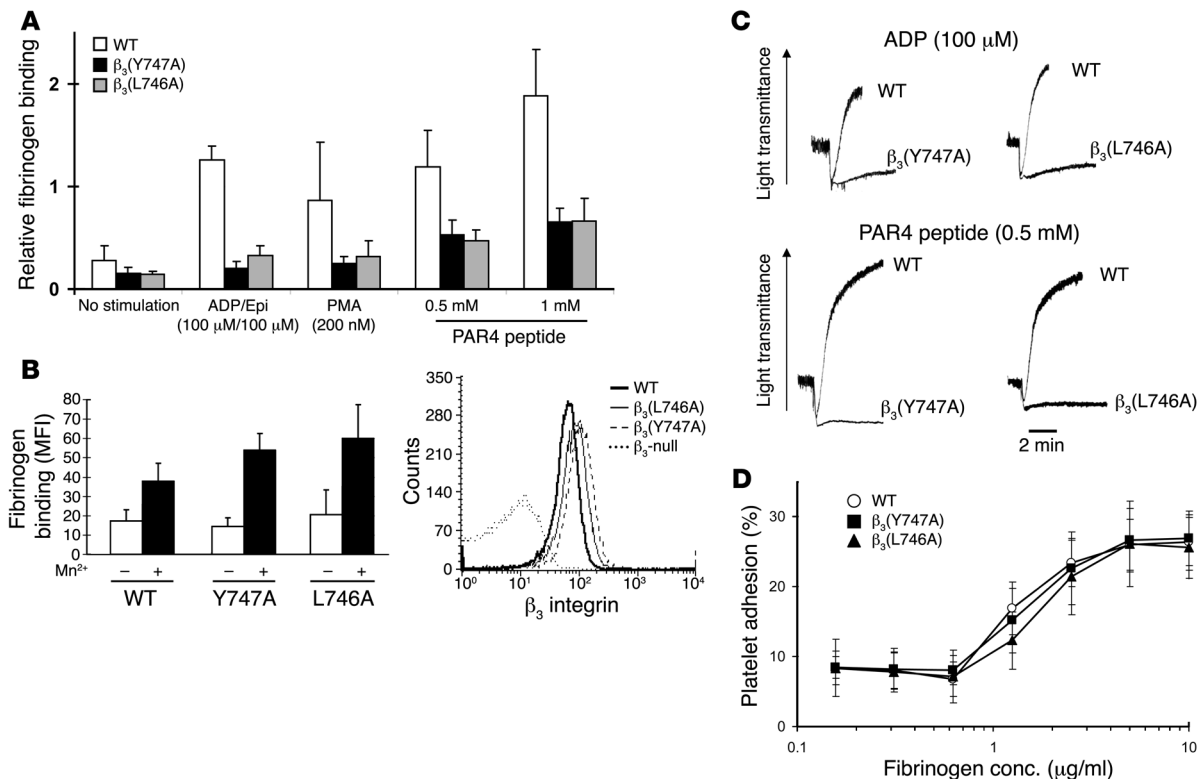


Figure 6

β_3 (Y747A) and β_3 (L746A) platelet interactions with fibrinogen. (A) FITC-labeled fibrinogen binding was measured by flow cytometry. Fibrinogen binding was reduced in β_3 mutant platelets in response to platelet agonists. Specific binding was defined as that which was inhibitable by 2 mM EDTA. Mean fluorescence intensity (MFI) for each agonist treatment was normalized to the MFI obtained with 0.5 mM MnCl₂ treatment. $n = 7, 6, \text{ and } 4$ for WT, β_3 (Y747A), and β_3 (L746A), respectively. Epi, epinephrine. (B) Platelets from both WT mice and β_3 mutants showed increased fibrinogen binding in the presence of 0.5 mM MnCl₂ (left). Surface β_3 integrin expression of platelets obtained from β_3 mutant animals (right). Results are representative of 4 independent experiments and at least 4 mice per genotype. (C) Aggregation of platelets obtained from WT or β_3 mutant mice was measured in response to the addition of 100 μ M ADP or 0.5 mM PAR4 peptide. Results are representative of at least 2 independent experiments on at least 3 animals from each genotype. (D) Platelet adhesion to immobilized fibrinogen. Washed platelets were incubated in fibrinogen-coated microtiter wells for 1 hour at room temperature. Results are shown as percentage of adherent cells relative to the total number added to each well. $n = 7, 5, \text{ and } 4$ for WT, β_3 (Y747A), and β_3 (L746A), respectively. Error bars represent SD.

to limit dosage to avoid pathological bleeding (5). Effective oral antithrombotics, such as aspirin or clopidogrel, partially block $\alpha_{IIb}\beta_3$ activation at the level of an agonist receptor or generation of an endogenous platelet agonist. Here we show that disrupting the β_3 integrin–talins interaction blocks $\alpha_{IIb}\beta_3$ activation and has a dramatic antithrombotic effect and that blocking this interaction leaves the ligand-binding function of platelet $\alpha_{IIb}\beta_3$ intact. Similarly, inhibiting $\alpha_{IIb}\beta_3$ activation by agents such as aspirin and clopidogrel also spares the ligand-binding function of $\alpha_{IIb}\beta_3$. This preservation of ligand-binding function in combination with preservation of outside-in signaling probably accounts for the markedly diminished pathological bleeding in the β_3 (L746A) mice relative to those with complete lack of β_3 function. Thus, these studies suggest the principle that the reduction in pathological bleeding associated with blocking the $\alpha_{IIb}\beta_3$ -talins interaction creates a wider therapeutic window than that achieved by blocking extracellular ligand binding to $\alpha_{IIb}\beta_3$. Furthermore, by preventing a final common event leading to integrin activation, disrupting this interaction might prove more effective than currently available oral antiplatelet agents that block a single agonist pathway. Small molecule inhibitors of integrin cytoplasmic domain protein–protein interac-

tions are feasible (34), and the critical structural features of the talin–integrin interaction have been defined (13), suggesting that the principle established here may pave the way to development of a new class of antithrombotic agents.

Methods

Generation of β_3 (Y747A) and β_3 (L746A) knock-in mice. A 6-kb fragment of the β_3 integrin gene encompassing exons 14 and 15 was amplified from R1 ES cell genomic DNA by PCR and inserted into pBluescript, and its identity was verified by sequencing. Mutations (coding for L746A or Y747A) in exon 15 were inserted by splice-overlap PCR (35) and confirmed by sequencing. A targeting vector was constructed by inserting a phosphoglycerate kinase (PGK) promoter–driven Neo cassette flanked by loxP sequences into a HindIII site between exons 14 and 15 and a PGK–diphtheria toxin A cassette 5' to the β_3 sequence (Figure 2A). The targeting sequence was isolated from pBluescript by NotI restriction digestion, agarose gel purified, and electroporated into 129/SvJ ES cells at both the UCSD Transgenic Core Facility and the Fannie E. Rippel Transgenic Facility at the Massachusetts Institute of Technology (MIT). G418-resistant colonies were screened by PCR using primer A (5'-CACTTTGAGGTTTGAGGGTC-3') and primer B (5'-GCTGATCTCTAGAGTCGAC-3') as depicted in Figure 2A. Positive clones

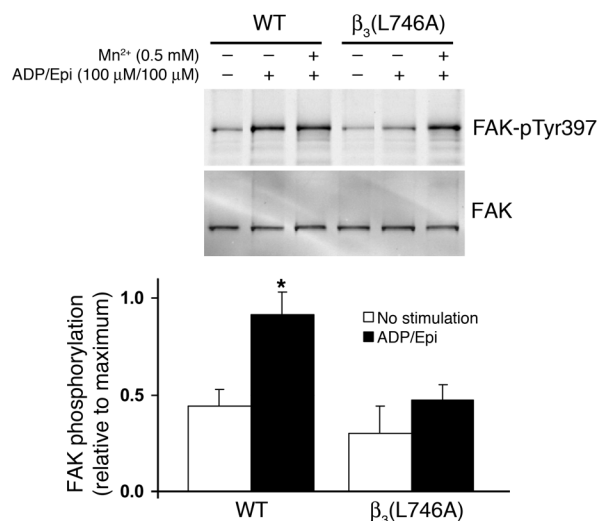


Figure 7

pp125^{FAK} phosphorylation. Platelets were incubated in suspension with 250 μg/ml soluble fibrinogen with or without 0.5 mM MnCl₂ and ADP/epinephrine (100 μM each), as indicated, for 20 minutes at room temperature. Platelets were lysed, and pp125^{FAK} phosphorylation was measured by immunoblotting using an antibody against pp125^{FAK} (pTyr397). Blots were stripped and reprobed with an antibody to pp125^{FAK}. Results are shown relative to maximum pp125^{FAK} phosphorylation signal for each group. **P* < 0.05.

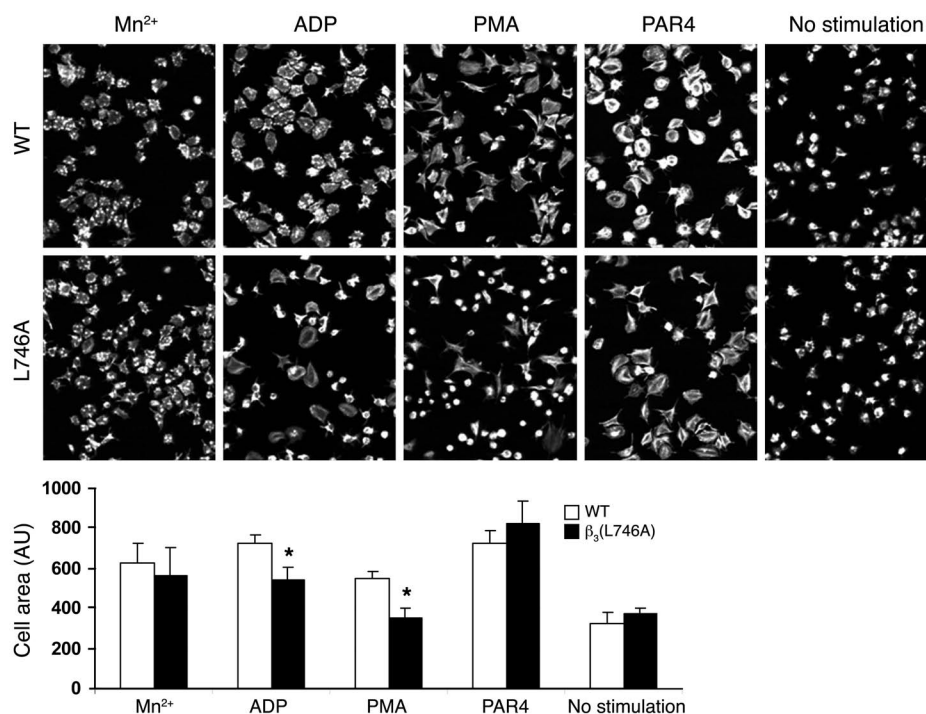
were further analyzed by Southern blotting of BamHI-digested genomic DNA using a 600-bp 5' cDNA probe upstream of the targeted sequence (Figure 2A). This resulted in a 3.2-kb band from the WT allele and a 5.4-kb band from the targeted allele. When genomic DNA was digested with EcoRI and hybridized with a 600-bp 3' cDNA probe complementary to a sequence downstream of the targeted sequence, we expected a 7-kb band from the WT allele and a 9.2-kb band from the targeted allele (Figure 2). Blots were hybridized with a cDNA containing the Neo resistance gene to detect random insertional events of the targeting vector. Positive clones (6 for each mutation), containing a single insertion, were karyotyped, and at least 2 clones for each mutant were injected into C57BL/6 host blastocysts. Chimeric male mice were bred to C57BL/6 females, and agouti offspring from these crosses were genotyped by PCR using genomic DNA extracted from ear biopsies and primer C (5'-CAGTCCTCTACCTTA-

CAGTG-3') and primer D (5'-CTCTGCCCTCAGTTTCCTTA-3') as depicted in Figure 2A. Two independently derived heterozygous animals for each mutation [β₃(Y747A), 1 from MIT and 1 from UCSD; and β₃(Y746A), from UCSD], were crossed with EIIa-Cre mice (The Jackson Laboratory) to delete the Neo cassette in germ cells (36). Deletion of Neo and presence of the targeted allele in offspring from β₃ mutant and EIIa-Cre crosses were evaluated by PCR of genomic DNA using primers C and D (Figure 2A). All experiments were performed with independently derived lines for each mutation that were backcrossed to the C57BL/6 strain for at least 3 generations. Sex-matched WT littermates were used as control animals. Mice were housed in the UCSD animal facility, and experiments were approved by the UCSD Institutional Animal Care and Use Committee.

Molecular modeling. Modeling was performed using DeepView — Swiss-Pdb viewer (<http://www.expasy.org/spdbv/>; ref. 37). β₃ integrin cytoplasmic

Figure 8

Agonist-stimulated platelet spreading. Platelets were allowed to spread on fibrinogen-coated coverslips (100 μg/ml) in the presence of MnCl₂ (0.5 mM), ADP (100 μM), PMA (200 nM), or PAR4 peptide (1 mM), as indicated, for 45 minutes, fixed, and stained with rhodamine-phalloidin. The results were quantified from 2 independent experiments. **P* < 0.05. Error bars represent SD. Original magnification, ×1,260.





domain interactions with filamin A were modeled based on the structure of β_7 integrin cytoplasmic domain and filamin A (38). This approach is justified by nuclear magnetic resonance spectroscopy and mutational studies that indicate that these integrin cytoplasmic domains bind to filamin A in a similar manner. Sequence threading was guided using the NPXY motif sequence, which is identical in the β_3 and β_7 integrins. The resulting sequence alignment was submitted to Swiss-Model (<http://swissmodel.expasy.org>). The resulting model had no major errors as determined by the WhatCheck report on the expasy website.

Affinity chromatography with recombinant integrin cytoplasmic domains. Platelets were obtained from WT C57BL/6 mice as described below and lysed as previously described (11). Affinity chromatography was performed using recombinant integrin cytoplasmic domains bound to His-Bind Resin (Novagen) as previously described (11, 14). Samples were separated on a 4%–20% SDS-polyacrylamide gel (Novex; Invitrogen) and transferred for Western blotting with the following antibodies: talin 8d4 (Sigma-Aldrich), anti-filamin A (a kind gift from John Hartwig, Harvard Medical School, Boston, Massachusetts, USA), and c-Src and Syk (Santa Cruz Biotechnology Inc.). Signal was detected and results quantified using an Odyssey imaging system (LI-COR Biosciences).

Thrombosis assays. Pulmonary thromboembolism experiments were performed as described previously (39). Briefly, mice under isoflurane anesthesia were administered 200 μ l of saline containing 0.8 mg/kg collagen (Chrono-log Corp.) and 60 μ g/kg epinephrine via tail vein injection. Animals were monitored for death as determined by cessation of breathing for up to 30 minutes after injection. Lungs were removed, fixed overnight with 10% neutral buffered formalin, and embedded in paraffin. Sections were stained with H&E, and images were captured with a Leica DM LS microscope and Spot color digital camera (National Diagnostics).

Ferric chloride-induced thrombosis was induced as previously described (40) by applying a 1.2 \times 1.2-mm piece of filter paper soaked in 5% ferric chloride to each side of the common carotid artery of a mouse under isoflurane anesthesia. After 3 minutes, the filter paper was removed and the vessel was washed twice with saline. Flow through the carotid artery was monitored 2 minutes before injury and at least 30 minutes after removal of the ferric chloride using a 0.5 PSB Doppler flow probe and T402 flowmeter (Transonic Systems Inc.). Following the assay, the artery was ligated with sutures to stop the flow of blood, and the artery was removed, fixed in 3.7% formaldehyde, embedded in paraffin, sectioned, and stained with H&E.

Hemostasis assays. The presence of fecal blood was assessed with a guaiac-based hemocult detection assay (Helena Laboratories) on freshly obtained stool samples. Tail bleeding assays were performed by resecting 1 mm of the tail followed by immersion in 37°C isotonic saline (17). All experiments were terminated at 10 minutes by cauterizing the tail.

Blood counts. Peripheral blood was collected from the retro-orbital plexus and transferred to tubes containing EDTA. Cell counts were performed using an MS9 automated cell counter (Melet Schloesing Laboratories) with veterinary parameters and reagents. Differential counts were performed manually on Wright-Giemsa-stained smears. Box-and-whisker plots of hemoglobin concentration were generated in which the box represents an interquartile range (IQR), a horizontal line represents the median, and vertical lines represent 1.5 \times IQR. Outliers are represented by filled circles and were included in statistical analysis.

Platelet isolation and functional assays. Washed platelets were obtained from fresh anticoagulated blood and resuspended at 3 \times 10⁸/ml in a platelet incu-

bation buffer (41). Soluble fibrinogen binding was performed by incubating platelets for 20 minutes with 150 μ g/ml FITC-labeled fibrinogen followed by fixation with 1% formaldehyde for 10 minutes at room temperature and analyzed on a FACScan (BD). Surface expression of β_3 integrin was measured by flow cytometry using an FITC-conjugated anti-mouse CD61 antibody (BD Biosciences). Platelet aggregation was performed as described previously (17) using platelet-rich plasma (PRP) at a platelet concentration of 3.5 \times 10⁸ platelets/ml obtained from blood drawn into 0.1-volume 0.13 M sodium citrate. Aggregation of 300 μ l of PRP was measured at 37°C while stirring using a 2-channel aggregometer (Chrono-log Corp.). Platelet adhesion assays were performed by incubating washed platelets for 1 hour at room temperature in fibrinogen-coated microtiter wells as previously described (42), and platelets were quantified by acid phosphatase assay (41). Platelet spreading was analyzed by confocal microscopy after cells were plated on coverslips coated with 100 μ g/ml fibrinogen for 45 minutes at room temperature. Platelets were fixed with 4% formaldehyde/PBS for 10 minutes at room temperature and labeled with rhodamine-phalloidin. Images were captured with a Leica SP2 confocal microscope, and cell area was quantified using ImageJ software (version 1.36b; <http://rsb.info.nih.gov/ij/>). To analyze FAK phosphorylation, platelets in suspension were incubated with 250 μ g/ml fibrinogen with or without 0.5 mM MnCl₂ and ADP/epinephrine (100 μ M each) for 20 minutes at room temperature. Platelets were then lysed by addition of one-half volume 3 \times lysis buffer (3% NP-40, 450 mM NaCl, 150 mM Tris-HCl, pH 7.4, 3 mM NaVO₄, 1.5 mM NaF, 3 mM PMSF, 15 mM EDTA, and complete protease inhibitor; Roche) and clarified by centrifugation at 13,000 g for 10 minutes at 4°C. Forty micrograms of protein was separated on 4%–20% Tris-glycine gels (Novex; Invitrogen) and transferred to nitrocellulose membranes for probing with anti-FAK(pTyr397) (Biosource) and FAK antibodies (Santa Cruz Biotechnology Inc.). Signal was detected and results quantified by infrared fluorescence spectrometry using an Odyssey imaging system (LI-COR Biosciences).

Statistics. Statistical significance was determined by Student's *t* test for all experiments but the pulmonary thromboembolism study, which was analyzed using Fisher's exact test. A *P* value of less than 0.05 was considered statistically significant.

Acknowledgments

We gratefully acknowledge Aurora Burds Connor and Ella Kotheri for excellent assistance in generating gene-targeted animals. We thank Zaverio Ruggeri for valuable discussions concerning the ferric chloride thrombosis model. This work was supported by grants from the NIH (HL57900 and HL078784) and from the Cell Migration Consortium, NIH (U54 GM064346). B.G. Petrich is a postdoctoral fellow of the American Heart Association. A.W. Partridge held a postdoctoral fellowship from the Tobacco-Related Disease Research Program. P. Fogelstrand has a postdoctoral fellowship from the Swedish Research Council.

Received for publication November 21, 2006, and accepted in revised form April 24, 2007.

Address correspondence to: Mark H. Ginsberg, Department of Medicine, University of California, San Diego, 9500 Gilman Drive, mail stop 0726, La Jolla, California 92093-0726, USA. Phone: (858) 822-6432; Fax: (858) 822-6458; E-mail: mhginsberg@ucsd.edu.

1. Quinn, M.J., Byzova, T.V., Qin, J., Topol, E.J., and Plow, E.F. 2003. Integrin α IIb β 3 and its antagonism. *Arterioscler. Thromb. Vasc. Biol.* **23**:945–952.
2. Chew, D.P., Bhatt, D.L., Sapp, S., and Topol, E.J. 2001. Increased mortality with oral platelet gly-

- coprotein IIb/IIIa antagonists: a meta-analysis of phase III multicenter randomized trials. *Circulation*. **103**:201–206.
3. Shattil, S.J., and Newman, P.J. 2004. Integrins: dynamic scaffolds for adhesion and signaling in

platelets. *Blood*. **104**:1606–1615.

4. Ginsberg, M.H., Partridge, A., and Shattil, S.J. 2005. Integrin regulation. *Curr. Opin. Cell. Biol.* **17**:509–516.
5. Bhatt, D.L., and Topol, E.J. 2003. Scientific and



- therapeutic advances in antiplatelet therapy. *Nat. Rev. Drug Discov.* **2**:15–28.
6. Liddington, R.C., and Ginsberg, M.H. 2002. Integrin activation takes shape. *J. Cell Biol.* **158**:833–839.
7. Adair, B.D., et al. 2005. Three-dimensional EM structure of the ectodomain of integrin $\alpha V\beta 3$ in a complex with fibronectin. *J. Cell Biol.* **168**:1109–1118.
8. Campbell, I.D., and Ginsberg, M.H. 2004. The talin-tail interaction places integrin activation on FERM ground. *Trends Biochem. Sci.* **29**:429–435.
9. Xiao, T., Takagi, J., Collier, B.S., Wang, J.H., and Springer, T.A. 2004. Structural basis for allostery in integrins and binding to fibrinogen-mimetic therapeutics. *Nature* **432**:59–67.
10. Calderwood, D.A., et al. 2002. The phosphotyrosine binding-like domain of talin activates integrins. *J. Biol. Chem.* **277**:21749–21758.
11. Calderwood, D.A., et al. 1999. The Talin head domain binds to integrin beta subunit cytoplasmic tails and regulates integrin activation. *J. Biol. Chem.* **274**:28071–28074.
12. Tadokoro, S., et al. 2003. Talin binding to integrin beta tails: a final common step in integrin activation. *Science* **302**:103–106.
13. Garcia-Alvarez, B., et al. 2003. Structural determinants of integrin recognition by talin. *Mol. Cell.* **11**:49–58.
14. Pfaff, M., Liu, S., Erle, D.J., and Ginsberg, M.H. 1998. Integrin beta cytoplasmic domains differentially bind to cytoskeletal proteins. *J. Biol. Chem.* **273**:6104–6109.
15. Ulmer, T.S., Yaspan, B., Ginsberg, M.H., and Campbell, I.D. 2001. NMR analysis of structure and dynamics of the cytosolic tails of integrin alpha IIb beta 3 in aqueous solution. *Biochemistry* **40**:7498–7508.
16. Law, D.A., et al. 1999. Integrin cytoplasmic tyrosine motif is required for outside-in alphaIIb beta3 signalling and platelet function. *Nature* **401**:808–811.
17. Hodivala-Dilke, K.M., et al. 1999. $\beta 3$ -integrin-deficient mice are a model for Glanzmann thrombasthenia showing placental defects and reduced survival. *J. Clin. Invest.* **103**:229–238.
18. Savage, B., Shattil, S.J., and Ruggeri, Z.M. 1992. Modulation of platelet function through adhesion receptors. A dual role for glycoprotein IIb-IIIa (integrin alpha IIb beta 3) mediated by fibrinogen and glycoprotein Ib-von Willebrand factor. *J. Biol. Chem.* **267**:11300–11306.
19. Wang, R., Shattil, S.J., Ambruso, D.R., and Newman, P.J. 1997. Truncation of the cytoplasmic domain of $\beta 3$ in a variant form of Glanzmann thrombasthenia abrogates signaling through the integrin $\alpha_{IIb}\beta_3$ complex. *J. Clin. Invest.* **100**:2393–2403.
20. Chen, Y.P., et al. 1992. Ser-752→Pro mutation in the cytoplasmic domain of integrin beta 3 subunit and defective activation of platelet integrin alpha IIb beta 3 (glycoprotein IIb-IIIa) in a variant of Glanzmann thrombasthenia. *Proc. Natl. Acad. Sci. U. S. A.* **89**:10169–10173.
21. Liu, S., Calderwood, D.A., and Ginsberg, M.H. 2000. Integrin cytoplasmic domain-binding proteins. *J. Cell Sci.* **113**:3563–3571.
22. Ma, Y.Q., et al. 2006. Regulation of integrin alphaIIb beta3 activation by distinct regions of its cytoplasmic tails. *Biochemistry* **45**:6656–6662.
23. Chen, Y.P., O'Toole, T.E., Ylanne, J., Rosa, J.P., and Ginsberg, M.H. 1994. A point mutation in the integrin beta 3 cytoplasmic domain (S752→P) impairs bidirectional signaling through alpha IIb beta 3 (platelet glycoprotein IIb-IIIa). *Blood* **84**:1857–1865.
24. Ylanne, J., et al. 1993. Distinct functions of integrin alpha and beta subunit cytoplasmic domains in cell spreading and formation of focal adhesions. *J. Cell Biol.* **122**:223–233.
25. Kim, M., Carman, C.V., and Springer, T.A. 2003. Bidirectional transmembrane signaling by cytoplasmic domain separation in integrins. *Science* **301**:1720–1725.
26. Kuo, J.C., Wang, W.J., Yao, C.C., Wu, P.R., and Chen, R.H. 2006. The tumor suppressor DAPK inhibits cell motility by blocking the integrin-mediated polarity pathway. *J. Cell Biol.* **172**:619–631.
27. Chen, H., et al. 2006. In vivo beta1 integrin function requires phosphorylation-independent regulation by cytoplasmic tyrosines. *Genes Dev.* **20**:927–932.
28. Czuchra, A., Meyer, H., Legate, K.R., Brakebusch, C., and Fassler, R. 2006. Genetic analysis of beta1 integrin “activation motifs” in mice. *J. Cell Biol.* **174**:889–899.
29. George, J.N., Caen, J.P., and Nurden, A.T. 1990. Glanzmann's thrombasthenia: the spectrum of clinical disease. *Blood* **75**:1383–1395.
30. Smyth, S.S., Reis, E.D., Vaananen, H., Zhang, W., and Collier, B.S. 2001. Variable protection of beta 3-integrin-deficient mice from thrombosis initiated by different mechanisms. *Blood* **98**:1055–1062.
31. Tahliliani, P.D., Singh, L., Auer, K.L., and LaFlamme, S.E. 1997. The role of conserved amino acid motifs within the integrin beta3 cytoplasmic domain in triggering focal adhesion kinase phosphorylation. *J. Biol. Chem.* **272**:7892–7898.
32. Woodside, D.G., et al. 2001. Activation of Syk protein tyrosine kinase through interaction with integrin beta cytoplasmic domains. *Curr. Biol.* **11**:1799–1804.
33. Collier, B.S. 2001. Anti-GPIIb/IIIa drugs: current strategies and future directions. *Thromb. Haemost.* **86**:427–443.
34. Ambroise, Y., Yaspan, B., Ginsberg, M.H., and Boger, D.L. 2002. Inhibitors of cell migration that inhibit intracellular paxillin/alpha4 binding: a well-documented use of positional scanning libraries. *Chem. Biol.* **9**:1219–1226.
35. Ho, S.N., Hunt, H.D., Horton, R.M., Pullen, J.K., and Pease, L.R. 1989. Site-directed mutagenesis by overlap extension using the polymerase chain reaction. *Gene* **77**:51–59.
36. Lakso, M., et al. 1996. Efficient in vivo manipulation of mouse genomic sequences at the zygote stage. *Proc. Natl. Acad. Sci. U. S. A.* **93**:5860–5865.
37. Guex, N., and Peitsch, M.C. 1997. SWISS-MODEL and the Swiss-PdbViewer: an environment for comparative protein modeling. *Electrophoresis* **18**:2714–2723.
38. Kiema, T., et al. 2006. The molecular basis of filamin binding to integrins and competition with talin. *Mol. Cell.* **21**:337–347.
39. DiMinno, G., and Silver, M.J. 1983. Mouse antithrombotic assay: a simple method for the evaluation of antithrombotic agents in vivo. Potentiation of antithrombotic activity by ethyl alcohol. *J. Pharmacol. Exp. Ther.* **225**:57–60.
40. Konstantinides, S., Schafer, K., Thinnies, T., and Loskutoff, D.J. 2001. Plasminogen activator inhibitor-1 and its cofactor vitronectin stabilize arterial thrombi after vascular injury in mice. *Circulation* **103**:576–583.
41. Law, D.A., et al. 1999. Genetic and pharmacological analyses of Syk function in alphaIIb beta3 signaling in platelets. *Blood* **93**:2645–2652.
42. Arias-Salgado, E.G., et al. 2005. PTP-1B is an essential positive regulator of platelet integrin signaling. *J. Cell Biol.* **170**:837–845.